Phosphorus doping of boron carbides

T. L. Aselage, D. Emin, G. A. Samara, D. R. Tallant, S. B. Van Deusen, M. O. Eatough, H. L. Tardy, and E. L. Venturini
Sandia National Laboratories, Albuquerque, New Mexico 87185

S. M. Johnson
SRI International, Menlo Park, California 94025
(Received 4 February 1993)

Substitution of an electron donor such as phosphorus for a carbon or boron atom in *p*-type semiconducting boron carbides is expected to reduce the hole concentration. Phosphorus-doped boron carbide samples have been prepared by hot isostatic pressing with homogeneous dopant levels of up to one phosphorus atom per ten unit cells. Raman spectroscopy and x-ray diffraction confirm the presence of phosphorus within two-atom intericosahedral chains. The high-temperature dc conductivities of doped samples were substantially lower than those of undoped boron carbides. This effect was due to a combination of reduced carrier concentrations and increased hopping activation energies. The low-temperature ac conductivity of doped samples is also smaller than that of undoped samples. However, the number of carriers participating in the ac conduction is a very small fraction ($<0.1\%$) of the total carrier density.

INTRODUCTION

The anomalously large Seebeck coefficients of boron carbides and the unexpectedly low thermal conductivities combine with moderate, thermally activated electrical conductivities to produce attractive thermoelectric figures of merit at very high temperatures.[1,2] With melting temperatures above 2400 °C, boron carbides offer the potential for thermoelectric power generation at temperatures significantly greater than those possible with Si/Ge alloys. Boron carbides are intrinsically *p*-type conductors. In this paper, we describe our initial attempts to prepare *n*-type boron carbides by phosphorus doping, with a focus on the location of phosphorus within the structure of the boron carbide and the electrical transport properties of the doped samples.

The ideal B_4C structure, shown in Fig. 1, comprises twelve-atom, boron-rich icosahedra and three-atom chains. Each of the icosahedra in B_4C contains a single carbon atom, $B_{11}C$, and each of the chains has a carbon atom at either end and a central boron atom, CBC.[3] The 15-atom unit cell thus contains 12 boron atoms and three carbon atoms, for an overall B_4C stoichiometry. Each $B_{11}C$ icosahedron has an affinity for an additional electron, which is donated by the twofold-coordinated boron atom of the chain.[3,4] This ideal $B_{12}C_3$ structure $(B_{11}C)^-[CB^+C]$ should be an electrical insulator.[4] Single-phase boron carbide samples, however, always have less carbon than this ideal $B_{12}C_3$ structure.[3,5] The single-phase region extends from about 9–19 at. % carbon, or $B_{12+y}C_{3-y}$, with y between 0.15 and 1.65. In carbon-saturated boron carbide, with $y \approx 0.15$, CBB chains replace about 15% of the CBC chains. Because a CBB chain is isoelectronic with a CB^+C chain, it does not donate an electron to an icosahedron.[4] The presence of CBB chains thus produces holes. Rather than quasifree band conduction, however, boron carbides manifest hopping conduction consistent with the formation and motion of small bipolaronic holes. These bipolarons are believed[4] to be associated with positively charged, carbon-containing icosahedra: $(B_{11}C)^+$. Since two electrons must be removed from a $(B_{11}C)^-$ to form each $(B_{11}C)^+$, two CBB chains are required to produce a single $(B_{11}C)^+$ icosahedron. With approximately 15% of the unit cells having CBB chains at 19 at. % carbon, the density of bipolaronic holes corresponds to about 7.5% of the unit cells. The unit-cell density obtained from the lattice constants of the boron carbides[6] is about $3\times10^{21}/cm^3$, so that the carrier density of carbon-saturated samples is about $2.2\times10^{20}/cm^3$.

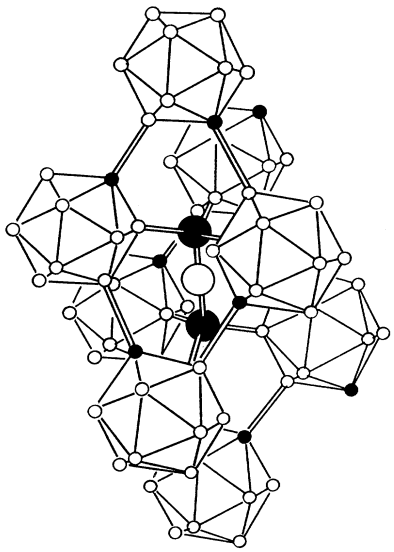

FIG. 1. Crystal structure of boron carbide with an ideal B_4C composition. Open circles represent boron atoms, whereas filled circles represent carbon atoms. Carbon atoms within icosahedra are not ordered.

0163-1829/93/48(16)/11759(8)/$06.00

Boron carbides are intrinsically *p*-type conductors for all compositions within the single-phase region. An efficient *n*-type complement to boron carbide is desired for thermoelectric applications. Previous attempts to prepare *n*-type boron carbides have focused on very low carbon concentrations[7] or on the incorporation of metal atoms.[8] Although a negative Hall constant was observed at room temperature in a sample with very low carbon content,[7] the sample was multiphase and thermally unstable. Since the carrier density of the boron carbide is smallest at the carbon-rich end of the solid solution, an alternate approach to producing *n*-type boron carbides is to substitute an electron donor into a carbon-saturated boron carbide.

Phosphorus was chosen as the "dopant" atom because of the existence of a boron phosphide, $B_{12}P_2$, that is structurally similar to boron carbide.[9] The $B_{12}P_2$ structure is obtained by replacing the three-atom chain of Fig. 1 with two phosphorus atoms. In $B_{12}P_2$, each icosahedron contains only boron. Phosphorus is precluded from occupying an icosahedral site due to its large size relative to a boron atom. Because of this structural similarity between $B_{12}P_2$ and boron carbides, it is anticipated that phosphorus, if at all soluble in boron carbide, will substitute at a chain position.

EXPERIMENTAL DETAILS

Samples of phosphorus-doped boron carbide were prepared by hot isostatic pressing (HIP). Mixtures of boron, carbon, and BP powders in batch compositions corresponding to $(B_{11}C)[CBC_{1-x}P_x]$ were pressed into pellets and sealed within evacuated fused silica ampoules. BP is thermally unstable at high temperatures, yielding phosphorus vapor and $B_{12}P_2$.[10] The use of BP as the phosphorus source allowed for the mixtures to be heated to a substantial fraction of the densification temperature without generating a large internal pressure. Subsequent decomposition of the BP provided a uniform source of phosphorus vapor. BN powder served as a buffer between the silica and boron carbide to minimize Si contamination of the samples. The ampoules were heated at 20 ° per min to 1800 °C in a HIP. An inert gas pressure of 100 psi was applied at 600 °C. With the quartz softened at 1800 °C, the inert gas pressure was increased to 29 000 psi as the temperature was increased at 10 ° per min to 1900 °C. After holding at 1900 °C and 29 000 psi for 2 h, samples were cooled to 300 °C and the pressure reduced to 10 000 psi over a period of 30 min. At 300 °C, the remaining pressure was removed and the samples cooled to room temperature.

After removal from the quartz enclosures, samples were ground to roughly 2-cm cubes. Samples were characterized by x-ray diffraction, Raman spectroscopy, and electron probe microanalysis (EPMA). X-ray-diffraction data were collected using a Siemens D500 automated diffractometer with Cu $K\alpha$ radiation. Internal and external Si powder standards were used for lattice-constant determination in powder and bulk samples, respectively. Raman spectra were acquired using a computer-controlled, scanning double monochromator with a cooled, photon-counting detector. The monochromator resolution was 6 cm^{-1} full width at half maximum. Samples were illuminated with the 514.5-nm wavelength from an argon-ion laser, which was focused to an approximately 2 mm by 0.1 mm line. The resulting spectra were fitted with exponential and polynomial functions to remove Rayleigh scatter and broad fluorescence features. The spectra have been scaled for presentation so that the intensities of the most intense Raman bands are the same.

Samples were prepared in three batches with the following phosphorus levels: batch I—$x=0.05$, 0.10; batch II—$x=0.20$, 0.35, 0.50; and batch III—$x=0.10$, 0.15, 0.20, 0.25. Of these, only samples from batch I were of good quality. Unless otherwise noted, data presented in this paper will be from batch I samples only. Samples from batch II were cracked and a second $B_{12}P_2$ phase was present. Batch III samples had high (up to 0.7 at. %) silicon contamination and very low phosphorus content, suggesting a breach in the sample enclosure. Figure 2 shows a backscattered electron image and phosphorus x-ray mapping of the batch I sample with $x=0.10$. Low porosity and absence of cracking is evident in Fig. 2. The phosphorus map shows that the dopant is uniformly distributed in the boron carbide matrix. Similar results were found in the $x=0.05$ sample. Quantitative analysis by EPMA showed homogeneous phosphorus concentrations of 0.32 and 0.61 at. %, compared to batch values of 0.33 and 0.67 at. % ($x=0.05$, 0.10), in these samples. Si impurities (from the SiO_2 enclosure) were found at a level of about 0.15 at. % in both batch I samples. Occasional small mottled regions on the surface of these samples were associated with regions of lower density. EPMA showed the matrix phase in these regions to be of the same composition as the bulk. Raman spectra obtained from such regions revealed the presence of some BN, which presumably hindered local densification.

Slabs of about 1.5-mm thickness, 5–8-mm width, and 15–20-mm length were cut from the larger cubes for electrical measurements. The dc electrical conductivity was measured from room temperature to about 400 °C under

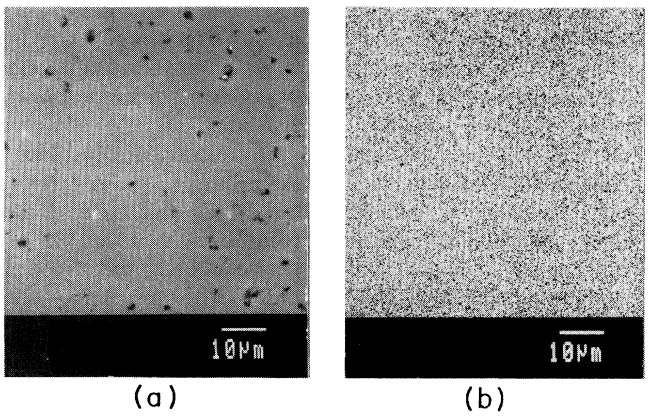

FIG. 2. (a) Backscattered electron image of a phosphorus-doped sample with $x=0.10$. (b) Phosphorus compositional x-ray mapping of the same region shown in (a). 10-μm scale bars are shown.

flowing gettered argon in a tube furnace fitted with a sealed alumina tube. Four-point measurements using painted gold contacts were employed. Seebeck measurements utilized sputtered Ti/Pt/Au electrodes, gold leads, and type-K thermocouples. After Ag paint and sputtered Au contacts gave evidence of parasitic capacitance in the low-temperature ac conductivity and dielectric measurements, sputtered Cr/Au contacts were deposited on the large parallel faces of the samples. These contacts adhered very well, gave accurate, reproducible, and reversible results, and showed no polarization or surface layer effects at low temperature. Parasitic capacitances were negligible with these contacts. The real and imaginary parts of the dielectric constants and ac conductivity were determined from complex impedance measurements performed as a function of temperature and frequency (10^2-10^5 Hz). These measurements were performed with the sample mounted in a helium gas-filled cell placed inside a conventional low-temperature cryostat.

Two-point conductivities using the Cr/Au contacts were compared to the four-point values near room temperature. The two point conductivities were significantly lower than those obtained with the four-point technique, indicating a significant contact resistance. Infrared reflectance spectra showed an OH stretching mode on the phosphorus-doped samples that is absent in undoped boron carbides. This mode and the contact resistance may both arise from hydrolysis of the phosphorus at the surface.

RESULTS

High-temperature, dc properties

The dc electrical conductivities (σ) of carbon-saturated boron carbides with phosphorus substitution in 5% and 10% of the unit cells ($x=0.05$ and 0.10) are plotted as σT versus the inverse temperature in Fig. 3. Also plotted are conductivity data for two undoped boron carbides with compositions of 19 at. % carbon (carbon-saturated) and about 18 at. % carbon. The temperature dependence of the conductivity of each of the samples is consistent with expectations for the adiabatic hopping of a temperature-independent number of small (bi) polarons.[4] Namely, the high-temperature conductivity is thermally activated, and the conductivity preexponential factor varies inversely with the temperature. This behavior has been observed in undoped boron carbides of all compositions within the single-phase region.[2,8,11,12] Phosphorus doping to levels of 10% of the unit cells does not change the apparent conduction mechanism.

The activation energies shown in Fig. 3 were determined by linear least-squares regression of the data obtained at temperatures above 400 K. The activation energy of each undoped sample, 170±2 meV, is characteristic of undoped boron carbides samples of all compositions.[2,8,11,12] The reduced conductivity evident in the phosphorus-doped sample is due in part to an increase in the hopping activation energy. The activation energy increases with the level of phosphorus doping: $E_A=222\pm2$ meV for $x=0.05$ and 240±2 meV for $x=0.10$. The relative effects of changes in carrier density and increases in the activation energy that accompany phosphorus doping will be discussed in detail below.

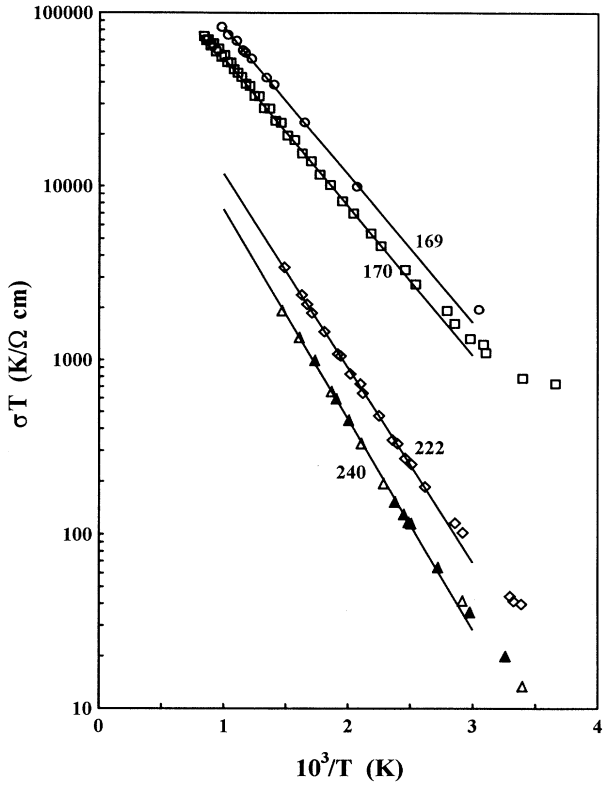

FIG. 3. Product of the dc conductivity σ and temperature T of undoped and phosphorus-doped boron carbides versus inverse temperature. ○: undoped, 18 at. % carbon; □: undoped, 19 at. % carbon; ◇: P doped, $x=0.05$; △, ▲: P doped, $x=0.10$, data from two slabs cut from the same sample. Solid lines are from linear least-squares fits to $T>400$ K data. The activation energies derived from such fits, in meV, are shown for each line.

The temperature dependence of the Seebeck coefficient of the $x=0.10$ sample is shown in Fig. 4. The conduction in this sample, with the highest homogeneous phosphorus content yet achieved, is still p type. The data are qualitatively similar to undoped boron carbide:[2,8,11,12] the Seebeck coefficient is large, with a small increase with temperature. This behavior in boron carbides has previously been attributed to bipolaronic hopping between inequivalent icosahedral sites.[4]

Low-temperature, ac properties

The response of a solid to an oscillating electric field is expressed in terms of the complex dielectric constant $\varepsilon=\varepsilon'-i\varepsilon''$. The conductivity $\sigma(\omega)$ is determined from the relationship $\sigma(\omega)=\omega\varepsilon''/4\pi$. We have measured the frequency dependence of the dielectric constant over the frequency range 10^2-10^5 Hz between 4 K and room temperature.

Above 77 K, the conductivities of the samples were not

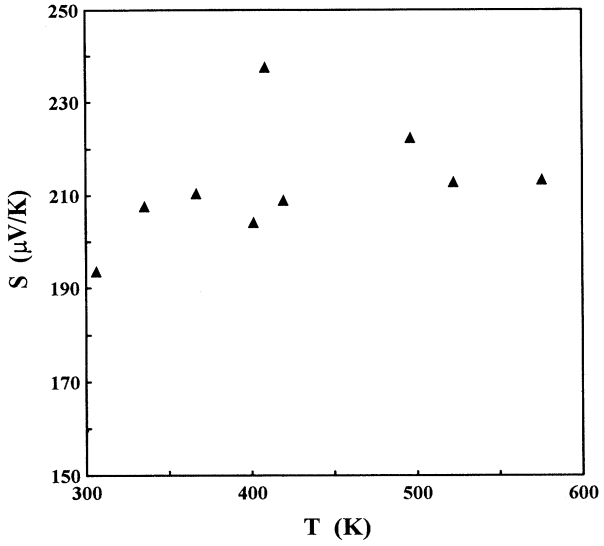

FIG. 4. Seebeck coefficient of a phosphorus doped boron carbide with $x=0.10$ as a function of temperature.

a function of the frequency, and $\sigma(\omega)\approx\sigma_{dc}$. At lower temperatures (≤ 30 K), however, $\sigma(\omega)$ is much larger than σ_{dc}, so that $\sigma(\omega)\approx\sigma_{ac}$. Figure 5 shows σ_{ac} over this temperature range at 10^3, 10^4, and 10^5 Hz for the phosphorus-doped sample with $x=0.05$ and for the undoped sample with 18 at. % carbon. The frequency and temperature dependences of the ac conductivities are qualitatively similar to those predicted by Emin[13] for adiabatic small-polaronic hopping between spatially close pairs of nearly degenerate sites. Like the high-temperature dc conductivity, the ac conductivity at a particular temperature and frequency decreases with increasing phosphorus concentration.

The real part of the dielectric constants ε' and the loss tangents $\tan\delta=\varepsilon''/\varepsilon'$ of both phosphorus-doped samples and of the undoped sample with 18 at. % carbon are plotted as a function of temperature of Fig. 6. As the temperature decreases and the hopping motion of the charge carriers slows, the samples behave increasingly as low-loss dielectrics. The onset of dielectric loss occurs at progressively higher temperatures with increasing phosphorus content, reflecting the decrease in hopping conductivity with increased phosphorus doping.

The inset of Fig. 6 shows the frequency dependence of the dielectric constant at 4 K for each of the three samples. The dielectric constant of the undoped boron carbide sample shows a strong frequency dependence at 10^5 Hz. In our prior study[14,15] of the low-temperature ac properties of undoped boron carbides, the carbon-concentration dependence of the dielectric constant between 10^2 and 10^{10} Hz mirrored the carbon-concentration dependence of the carrier density. This result suggested that the primary contribution to polarization in this frequency range came from the carriers. Consistent with a reduction in carrier density with phosphorus doping, the low-frequency dielectric constants of the phosphorus-doped samples are smaller than the undoped boron carbide.

The high-frequency (10^{14} Hz) dielectric constant for

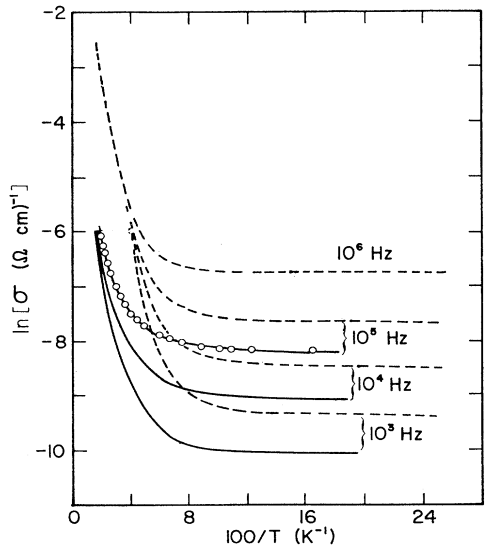

FIG. 5. ac conductivities of boron carbides between 10^3 and 10^6 Hz as a function of temperature — — —: undoped, 18 at. % carbon; ——: P doped, $x=0.05$.

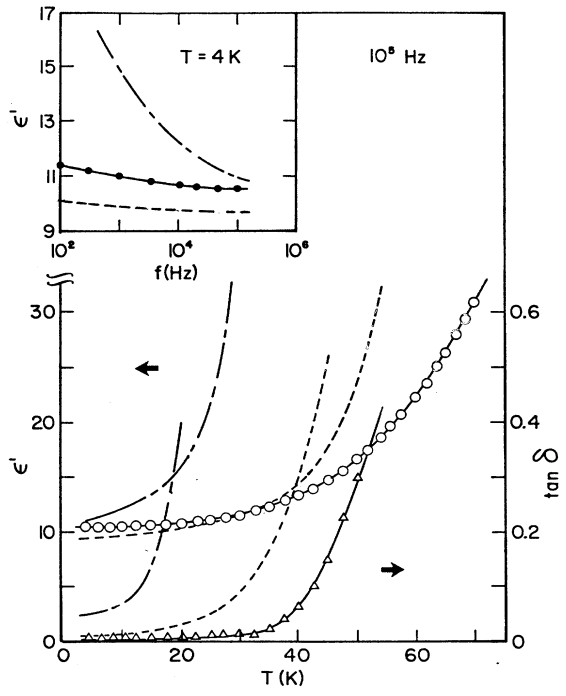

FIG. 6. Dielectric constants and loss tangents of boron carbides at 10^5 Hz vs temperature —·—·—: undoped, 18 at. % carbon; — — —: P doped, $x=0.05$; ——: P doped, $x=0.10$. Inset: Dielectric constants of these samples at 4 K as a function of frequency.

both phosphorus-doped samples was obtained by Kramers-Kronig analysis of reflectance spectra measured from 450 to 40 000 cm^{-1}. The experimental procedures and calculations have been described elsewhere.[16] The value found for both samples, 7.0 ± 0.5, is nearly identical to those obtained for undoped boron carbides.[14,15] The low-frequency dielectric constants of the phosphorus-doped samples in Fig. 6 appear to be approaching frequency-independent values of 9.4 and 10.3 for the $x=0.05$ and 0.10 samples, respectively. This frequency independence must yield to a decline in order to reach the high-frequency value of 7.0. Such a drop might be related to the freezing out with increasing frequency of interfacial polarization effects or of lattice modes associated with the phosphorus dopant.

Structural data

Raman spectroscopy has been used to study the effect of phosphorus incorporation on the structure of boron carbide. Previous analysis[17,18] of Raman spectra of undoped boron carbides as a function of composition and isotope resulted in the assignment of broad Raman bands at frequencies greater than 600 cm^{-1} to intericosahedral and intraicosahedral vibrations. Two narrow bands at about 480 and 534 cm^{-1} were attributed to vibrational modes involving CBC chains. The origin of broad bands at frequencies below 400 cm^{-1} is still uncertain. The intensities of such low-frequency bands differ considerably among different samples of the same bulk composition.

Raman spectra obtained from the homogeneous phosphorus-doped samples ($x=0.05$ and 0.10) and the boron carbide regions of the multiphase batch II samples (batch loadings of $x=0.20$ and 0.35) are compared with undoped boron carbide (19 at. % carbon) in Fig. 7. The high-frequency, icosahedral Raman bands in Fig. 7 show little change with phosphorus doping. The narrow bands centered at 500 cm^{-1}, however, show a progressive decrease in intensity with increasing levels of phosphorus doping. In addition to a decrease in intensity, the 481 cm^{-1} band progressively broadens with increasing phosphorus content.

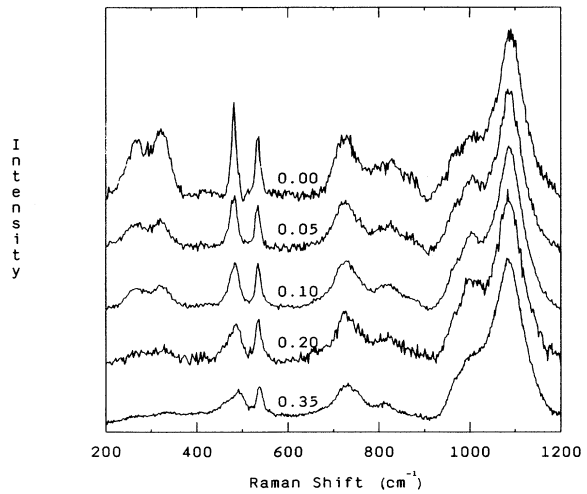

FIG. 7. Raman spectra of undoped boron carbide with 19 at. % carbon (labeled 0.00), homogeneous P-doped ($x=0.05$ and 0.10) boron carbides, and boron carbide regions of multiphase samples with higher phosphorus batch loadings ($x=0.20$ and 0.35). The phosphorus content of the boron carbide phase in the latter two samples is unknown.

The lattice constants of undoped boron carbide with 19 at. % carbon,[6] the homogeneous phosphorus-doped samples with $x=0.05$ and 0.10, and of the boron-carbide phase in the multiphase samples (batch II) are listed in Table I. The major effect of phosphorus doping is observed in the hexagonal c axes, which become shorter with increasing doping levels. The a axes of the homogeneous samples ($x=0.05$, 0.10) are nearly identical to undoped, carbon-saturated boron carbide. Higher phosphorus batch concentrations produce an increase in the a axis length.

The c axis of the hexagonal unit cell of boron carbides is parallel to the three-atom chain. Atomic substitutions within this chain might therefore be expected to notably affect the c axis. Substitution of silicon into the chain, forming a SiBC chain, results in an increase in the c axis length.[19] Similar results should be expected from a three-atom chain that incorporates phosphorus. Observation of exactly the opposite, a shortening of the c axis with increasing incorporation of phosphorus, argues for the formation of a two-atom, PB, PC, or PP chain. The decrease in intensity of the Raman bands centered at 500 cm^{-1} is consistent with the progressive replacement of symmetric CBC chains with two-atom, phosphorus-containing chains. This result, therefore, supports the previous assignment of the 480 and 534 cm^{-1} Raman bands in boron carbides to CBC chain-related vibrational modes.

Two-atom, PP chains are found in $B_{12}P_2$.[9] PB chains have been suggested in phosphorus-deficient $B_{12+x}P_{2-x}$ prepared by chemical vapor deposition[20] and by thermal decomposition of boron monophosphide.[21] Absorption bands at 610 and 338 cm^{-1} in the infrared spectrum of $B_{12+x}P_{2-x}$ were attributed to vibrations involving PB chains.[21] Infrared reflectance measurements of our $x=0.05$ and 0.10 samples above 500 cm^{-1} did not detect any new IR-active vibrational modes. However, the concentration of the two-atom chains in these samples is low

TABLE I. Lattice constants of phosphorus-doped boron carbides.

Batch composition x[a]	a (Å)	c (Å)
0.00[b]	5.599	12.070
0.05	5.589(3)	12.014(9)
0.10	5.598(3)	12.012(8)
0.20	5.608(2)	12.023(5)
0.35	5.614(2)	11.973(6)
0.50	5.627(1)	11.990(2)

[a]$(B_{11}C)[CBC_{1-x}P_x]$, bottom three entries are for multiphase samples.

[b]Data from Ref. 6. Standard deviations are listed in parentheses for lattice constants measured in this work.

compared to the concentration of icosahedral carbon atoms that are believed[3,22] to provide the predominant IR activity in boron carbides. Additionally, a weak absorption of boron carbide near 600 cm^{-1} may obscure any absorption due to PB or PC chains near this frequency.

DISCUSSION

The Raman spectra and lattice constants of phosphorus-doped boron carbides are consistent with the substitution of phosphorus in a chain site. As discussed above, the decreasing length of the c axis with increasing phosphorus concentration suggests the formation of two-atom, PB, PC, or PP chains. The interatomic separation of the PP chain in $B_{12}P_2$ is 2.24 Å. This distance is close to twice the covalent radius of phosphorus, suggesting a strong covalent bond between the phosphorus atoms in this chain. X-ray-diffraction studies find that the CBC chain in undoped boron carbides has a length of 2.86 Å. The decrease in the c axis length of the phosphorus-doped boron carbides in this study is only about 0.07 Å. Thus, the atoms of a PP chain in the lattice of boron carbide would be much farther apart than a normal covalent bond length, suggesting much weaker or no bonding between the phosphorus atoms. The symmetric stretching mode of the PP chain in $B_{12}P_2$ is Raman active, with a frequency of about 475 cm^{-1}. A much softer PP chain in boron carbides would have a lower vibrational frequency. No evidence of such a mode is observed in the Raman spectra of the doped samples. We therefore regard the presence of PP chains as unlikely at the phosphorus concentration levels of our doped samples.

Similarly, the sum of the covalent radii of phosphorus and carbon, 1.83 Å, or of phosphorus and boron, 1.88 Å, is considerably smaller than the distance between the two chain-end sites. This again suggests that the atoms of a PB or PC chain are not bonded to one another. Such nonbonded chain atoms are not without precedent in icosahedral borides: the oxygen atoms in $B_{12}O_2$ are also too far apart to bond to one another.[23]

Each of the atoms at the end of the chains is threefold coordinated to atoms of the three adjacent icosahedra. A phosphorus atom in such coordination will have two remaining valence electrons. These electrons may reside in a lone pair, or one or both electrons may be donated to the high-electron-affinity icosahedra. Similarly, carbon has a single extra valence electron, which may be donated to an icosahedron. Boron has its valence of three fulfilled by the trigonal chain-end coordination.

Donation of a single electron by a phosphorus would result in an unpaired electron associated with the phosphorus. Likewise, lack of donation by a carbon would also result in an unpaired electron. The spins associated with these unpaired electrons are detectable by magnetic susceptibility or electron spin resonance measurements. Undoped, carbon-saturated boron carbides have paramagnetic defect concentrations of about $1.5\times10^{19}/cm^3$.[24,25] It has been proposed that these defects are singly ionized carbon atoms at the center of CC^+C chains. Because the level of phosphorus doping is an order of magnitude larger than this intrinsic spin density, unpaired electrons at a phosphorus atom or carbon atom associated with phosphorus doping should be detectable. The temperature dependence of the magnetic susceptibility of the sample with $x=0.05$ was measured between 4 and 100 K and fit to a Curie-Weiss law ($\theta\approx0.9$ K). The density of spins deduced from this measurement, about $1\times10^{19}/cm^3$, is similar to the intrinsic density of spins in undoped boron carbides and an order of magnitude lower than the phosphorus concentration. Chain donation that results in an unpaired electron is thus excluded from further consideration.

The remaining possibilities for phosphorus incorporation within the chains, and the number of electrons donated per chain (in parentheses), are as follows: $\equiv P{:}C^+\equiv(1)$, $\equiv P^{2+}C^+\equiv(3)$, $\equiv P{:}B\equiv(0)$, and $\equiv P^{2+}B\equiv(2)$, where the symbol : represents a lone pair. The net increase in electron donation of these chains is obtained by subtracting the number of electrons donated by the chains that they replace, either CB^+C (1) or CBB (0). With these configurations, net electron donations of -1 to 3 electrons per phosphorus atom are, in principle, possible. Because of the high affinity of a positively charged icosahedron for electrons, unbonded lone pairs within the chains are likely to be a less favorable configuration than ionized chains with donation to the icosahedra. We therefore presume that donation occurs with a net increase of at least one electron per phosphorus atom. For donation to occur from a PP chain with no residual spins, each of the phosphorus atoms must donate both nonbonded valence electrons. The high Coulomb repulsion energy of such a P^{2+}-P^{2+} chain again suggests that formation of PP chains in doped boron carbides is unlikely.

The reduction in the carrier density due to such donation may be estimated from the high-temperature dc conductivities. The conductivity due to adiabatic small polaron hopping may be expressed as[4]

$$\sigma=(nq^2a^2\nu/kT)\exp(-E_A/kT)\ , \tag{1}$$

where n is the carrier density, q is the charge per carrier, a is the mean distance that a carrier hops, ν is a characteristic vibrational frequency, E_A is the activation energy, and k is the Boltzmann constant. The parameter $a^2\nu$ that enters into the prefactor of Eq. (1) is relatively insensitive to carbon concentration in undoped boron carbides. Indeed, substitution of experimental values of σ and E_A and carrier concentrations in accord with the structural model into Eq. (1) results in a physically reasonable value, $a^2\nu\approx0.2$ cm^2/sec.[2,4] Taking the ratio of the conductivity of undoped, carbon-saturated boron carbide to doped boron carbide and assuming that $a^2\nu$ is not appreciably changed by the phosphorus doping, we obtain after some rearrangement

$$\Delta n=n_u[1-(\sigma_d/\sigma_u)\exp\{(E_d-E_u)/kT\}]\ . \tag{2}$$

Here n_u, σ_u, and E_u are the carrier density, conductivity, and activation energy, respectively, of undoped boron carbide, σ_d and E_d are the conductivity and activation energy of the doped boron carbide, and Δn is defined as the decrease in bipolaron concentration due to the phos-

phorus doping, $\Delta n \equiv n_u - n_d$. Using the 600-K conductivities (Fig. 3) with $n_u = 2.2\times10^{20}/\text{cm}^3$, Eq. (2) results in Δn of $1.36\times10^{20}/\text{cm}^3$ ($x=0.05$) and $1.55\times10^{20}/\text{cm}^3$ ($x=0.10$). The net increase in the electron donation from the chains is twice the number of bipolaronic holes eliminated, $2\Delta n$. The net increase per phosphorus atom is then $2\Delta n$ divided by the concentration of the phosphorus dopant $(3\times10^{21}/\text{cm}^3)(x)$, where the density of unit cells is $3\times10^{21}/\text{cm}^3$ and x is the fraction of unit cells that contain a phosphorus atom. The net increase in donation per phosphorus atom is thus calculated to be 1.8 electrons ($x=0.05$) and 1.0 electron ($x=0.10$), in accord with expectations. These calculations ignore the effect of the silicon impurity in the samples. SiBC chains are found[19] in Si-doped boron carbides. A SiBC chain is capable of donating one electron to an icosahedron. If SiBC chains substitute for CBC chains, no net increase in electron donation occurs and the reduction in the bipolaronic hole concentration is due entirely to the phosphorus. If CBB chains are replaced, a net donation increase of one electron per SiBC chain is expected, and the number of electrons donated by a phosphorus calculated above is then an upper bound. Alternate preparation techniques to eliminate the Si impurity are being investigated.

The reduced conductivity in phosphorus-doped boron carbides results both from a reduction in carrier density due to charge donation from phosphorus-containing chains and from an increase in the hopping activation energy. The application of hydrostatic pressure to undoped boron carbides also results in an increase in the activation energy.[26] This effects results from the nature of the bonding in boron carbides. The stiffest bonds in the structure are the intericosahedral bonds and the bonds between the icosahedra and chains. The intraicosahedral bonds are relatively soft. Thus, boron carbides have been referred to as "inverted molecular solids."[27] Application of pressure results primarily in a compression of the icosahedra. Such a compression serves to deepen the potential wells that bind the carriers to their icosahedral sites, with the effect being an increase in the hopping activation energy. We propose that the increase in activation energy with phosphorus incorporation is due to a similar effect. In particular, the introduction of a large phosphorus atom at a chain-end position will compress icosahedra in the vicinity of the phosphorus atom. Application of pressure to the phosphorus-doped boron carbide samples also produced a decrease in the conductivity. Accurate measurements of the changes in activation energies were precluded due to the contact resistance problems associated with the two-point measurements.

The low-temperature ac conductivity of the phosphorus-doped boron carbides is also significantly lower than that of undoped samples. Emin[13] has recently shown that the ac conductivity observed in boron carbides[14,15] is consistent with that expected from the adiabatic hopping of small (bi)polarons between spatially close pairs of nearly degenerate sites. In particular, the primary contributions to σ_{ac} come from such pairs that respond at the frequency of the measurement. The polarization conductivity can be interpreted[13] as being the product of the number of such pairs at a particular frequency n_{pairs}, the carrier's charge, and its "mobility" in moving between sites at the forcing frequency ν

$$\sigma_{ac} = (n_{\text{pairs}})(q)(q\langle R^2\rangle\nu/kT) , \quad (3)$$

where R is the separation between sites. Taking this separation to be of the order of 10 Å, the number of pairs involved in the ac conductivity of undoped boron carbide with 18 at. % carbon at 6.1 K is about 3 to $6\times10^{16}\text{cm}^3$. The carrier density obtained from the high-temperature dc measurements, about $2\times10^{20}/\text{cm}^3$, is nearly four orders of magnitude larger. Thus, only a very small fraction of the carriers present in boron carbides participate in the low-temperature ac conduction. The number of pairs participating in the low-temperature ac conduction of the phosphorus-doped samples is even smaller. For example, at 6.1 K, $n_{\text{pairs}}(x=0.05)/n_{\text{pairs}}$ (18 at. % carbon) = 0.14 at 10^3 Hz, 0.18 at 10^4 Hz, and 0.23 at 10^5 Hz. In addition to reducing the total number of carriers, phosphorus doping may decrease the number of pairs involved in the ac conduction by reducing the occurrence of nearly degenerate pairs due to increasing disorder.

CONCLUSIONS

Phosphorus is soluble in boron carbides in concentrations of at least one atom per ten unit cells. The phosphorus dopant atom appears to be located at the ends of the chains in the boron carbide structure. The progressive reduction in the intensity of two narrow Raman bands centered at 500 cm^{-1} with incorporation of phosphorus within the chains confirms the previous association of these Raman modes with CBC chains. Both the high-temperature dc and low-temperature ac conductivities are reduced by phosphorus doping. Although the conduction is still p type, the dc results suggest a decrease of up to 70% in the density of bipolaronic holes compared to undoped samples. With a modest increase in dopant level, n-type conduction may prevail. The hopping activation energy is also greater for the phosphorus doped samples. This increase results from large phosphorus atoms compressing the relatively soft icosahedral sites that bind the carriers. The number of pairs involved in low-temperature ac conduction in boron carbides is less than 0.1% of the high-temperature carrier density. Nonetheless, introduction of phosphorus lowers the ac conductivity by reducing the total number of bipolaronic carriers and by increasing the disorder in the solid.

ACKNOWLEDGMENTS

The authors are grateful to Herman Stein for infrared reflectance measurements and to Paul Hlava for microprobe analysis. This work was supported by the Division of Materials Sciences, Office of Basic Energy Sciences of the U.S. DOE under contract No. DE-AC04-76DP00789.

[1]C. Wood, in *Boron-Rich Solids,* Proceedings of an International Conference on the Physics and Chemistry of Boron and Boron-Rich Borides, edited by D. Emin, T. Aselage, C. Beckel, I. Howard, and C. Wood, AIP Conf. Proc. No. 140 (AIP, New York, 1986), p. 362.

[2]T. L. Aselage, in *Modern Perspectives on Thermoelectrics and Related Materials,* edited by D. Allred, C. Vining, and G. Slack, MRS Symposia Proceedings No. 234 (Materials Research Society, Pittsburgh, 1991), p. 145.

[3]See T. L. Aselage and D. Emin, in *Boron-Rich Solids,* Proceedings of the 10th International Symposium on Boron, Borides, and Related Compounds, edited by D. Emin, T. Aselage, A. Switendick, B. Morosin, and C. Beckel, AIP, Conf. Proc. No. 231 (AIP, New York, 1991) p. 177.

[4]D. Emin, in *Boron-Rich Solids* (Ref. 1), p. 189.

[5]K. A. Schwetz and P. Karduck, in *Boron-Rich Solids* (Ref. 3), p. 405.

[6]T. L. Aselage and R. G. Tissot, J. Am. Ceram. Soc. **75**, 2207 (1992).

[7]A. N. Campbell, A. W. Mullendore, D. R. Tallant, and C. Wood, in *Novel Refractory Semiconductors,* edited by D. Emin, T. Aselage, and C. Wood, MRS, Symposia Proceedings No. 97 (Materials Research Society, Pittsburgh, 1987), p. 113.

[8]N. B. Elsner, G. H. Reynolds, J. H. Norman, and C. H. Shearer, in *Boron-Rich Solids* (Ref. 1), p. 59.

[9]B. Morosin, A. W. Mullendore, D. Emin, and G. A. Slack, in *Boron-Rich Solids* (Ref. 1), p. 70.

[10]F. V. Williams and R. A. Ruehrwein, J. Am. Chem. Soc. **82**, 1330 (1960); L. H. Spinar and C. C. Wang, Acta Crystallogr. **15**, 1048 (1962); J. L. Peret, J. Amer. Ceram. Soc. **47**, 44 (1964).

[11]C. Wood and D. Emin, Phys. Rev. B **29**, 4582 (1984).

[12]M. Bouchacourt and F. Thevenot, J. Mater. Sci. **20**, 1237 (1985).

[13]D. Emin, Phys. Rev. B **46**, 9419 (1992).

[14]G. A. Samara, H. L. Tardy, E. L. Venturini, T. L. Aselage, and D. Emin, Phys. Rev. B **48**, 1468 (1993).

[15]G. A. Samara, H. L. Tardy, E. L. Venturini, T. L. Aselage, and D. Emin, in *Boron-Rich Solids* (Ref. 3), p. 77.

[16]H. L. Tardy, T. L. Aselage, and D. Emin, in *Boron-Rich Solids* (Ref. 3), p. 138.

[17]D. R. Tallant, T. L. Aselage, A. N. Campbell, and D. Emin, Phys. Rev. B **40**, 5649 (1989).

[18]D. R. Tallant, T. L. Aselage, and D. Emin, in *Boron-Rich Solids* (Ref. 3), p. 301.

[19]R. Telle, in *The Physics and Chemistry of Carbides, Nitrides, and Borides,* Vol. 185 of *NATO Advanced Study Institute, Series B: Physics,* edited by R. Freer (Kluwer Academic, Dordrecht, 1990), p. 249.

[20]von E. Amberger and P. A. Rauh, Acta Crystallogr. B **30**, 2549 (1974).

[21]von H. J. Becher, F. Thevenot, and C. Brodhag, Z. Anorg. Allg. Chem. **469**, 7 (1980).

[22]H. J. Stein, T. L. Aselage, and D. Emin, in *Boron-Rich Solids* (Ref. 3), p. 322.

[23]H. Bolmgren, T. Lundstrom, and S. Okada, in *Boron-Rich Solids* (Ref. 3), p. 197; I. Higashi, M. Kobayashi, J. Bernhard, C. Brodhag, and F. Thevenot, in *Boron-Rich Solids* (Ref. 3), p. 201.

[24]E. L. Venturini, L. J. Azevedo, D. Emin, and C. Wood, in *Boron-Rich Solids* (Ref. 1), p. 292.

[25]E. L. Venturini, D. Emin, and T. L. Aselage, in *Novel Refractory Semiconductors* (Ref. 7), p. 57.

[26]G. A. Samara, D. Emin, and C. Wood, Phys. Rev. B **32**, 2315 (1985).

[27]D. Emin, in *Novel Refractory Semiconductors* (Ref. 7), p. 3.

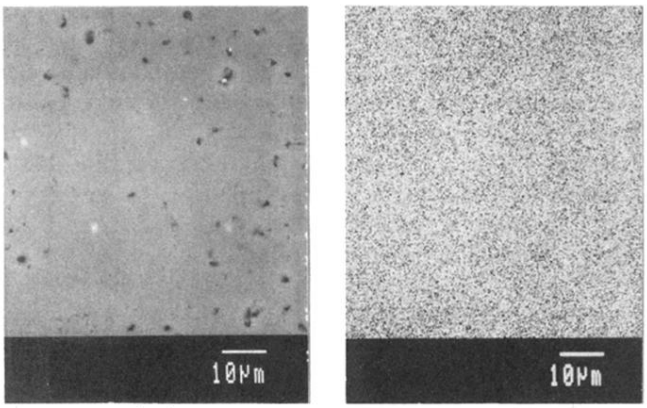

FIG. 2. (a) Backscattered electron image of a phosphorus-doped sample with $x=0.10$. (b) Phosphorus compositional x-ray mapping of the same region shown in (a). 10-μm scale bars are shown.